Journal of Ocean Engineering and Marine Energy (2020) 6:91–97
https://doi.org/10.1007/s40722-020-00160-0

SHORT COMMUNICATION

Application of a sea surface roughness formula using joint statistics of significant wave height and spectral wave steepness

Dag Myrhaug[1] · Bernt J. Leira[1] · Wei Chai[1]

Received: 2 September 2019 / Accepted: 28 January 2020 / Published online: 14 February 2020

Abstract
This article provides some statistical features of the sea surface roughness given as a function of the spectral wave steepness and the significant wave height suggested by Taylor and Yelland (J Phys Oceanogr 31:572–590, 2001), which is best to use for mixed wind sea and swell, and for swell-dominated situations (Drennan et al., J Phys Oceanogr 35:835–848, 2005). Results are obtained using the Myrhaug and Fouques (2008) bivariate statistics of the spectral wave steepness and the significant wave height representing wind sea, swell, and combined wind sea and swell. Associated results are also given for the sea surface drag coefficient and the turbulent energy density, as well as a procedure of estimating the sea surface roughness from 1-, 10- and 100-year contour lines. Finally, a simple example of application is given, demonstrating the effect of the sea surface roughness on slowly varying surge motion of marine structures exposed to wind gust.

Keywords Sea surface roughness · Significant wave height · Spectral wave steepness · Bivariate distributions · Contour lines · Logarithmic mean wind speed profile · Wind gust spectrum · Slowly varying surge motion

1 Introduction

The sea surface roughness depends on the mechanisms of air–sea interaction and its estimation is difficult; no consistent theory exists covering the range from small waves to big waves including wind waves, combined wind waves and swell, as well as swell. Charnock (1955) presented his formula based on a dimensional argument, i.e. the sea surface roughness $z_0 = \beta u_*^2/g$, where the original Charnock parameter is $\beta = 0.012$, and u_* is the friction velocity. Since then, many different values of β as well as formulae for z_0 have been proposed, also containing the wind speed as a parameter; see, e.g. Jones and Toba (2001) for a review.

Drennan et al. (2005) performed a comprehensive intercomparison of different parameterizations of the sea surface roughness using field data from eight locations ranging from lakes to deep-water sea. They found that if bulk sea state parameters such as significant wave height and spectral peak period are available, then the roughness formula as a function of the spectral wave steepness and the significant wave height proposed by Taylor and Yelland (2001) [see Eq. (1)] was the best to use for mixed wind sea and swell, and for swell-dominant situations (see Drennan et al. (2005) for more details). A recent review of the literature is provided by Zhao and Li (2019), followed by presenting results from a comprehensive analysis of the influence of wind waves on wind stress with respect to sea surface roughness and drag coefficient based on both laboratory and field data. In the pioneering work of Powell et al. (2003) and Zhao and Li (2019) it was found that the drag coefficient reaches a peak for strong winds, i.e. for wind speeds exceeding 30–40 m/s. Zhao and Li (2019) also found that a roughness formula in terms of the spectral wave steepness and the significant wave height can be applied to estimate wind stress from low to high winds (see Sect. 2). Myrhaug (2020) demonstrated how this sea surface roughness formula for wind sea can be applied to estimate the sea surface roughness based on wind and wave statistics.

Some recent works related to load assessment studies for offshore wind power systems have advocated the use of the Hsu (1974) relationship for z_0 where the sea surface roughness depends on the wave conditions, taking the Charnock parameter equal to the wave steepness s, i.e. $\beta = s = H/\lambda$, where H is the wave height and λ is the wave length. This

✉ Dag Myrhaug
dag.myrhaug@ntnu.no

[1] Department of Marine Technology, Norwegian University of Science and Technology (NTNU), Otto Nielsens vei 10, 7491 Trondheim, Norway

was adopted and used for shallow-water waves by Donkers et al. (2011) and Kalverla et al. (2017) as part of an extensive analysis of wind conditions in the Dutch part of the southern North Sea. Furthermore, Myrhaug (2018) presented some statistical properties of the deep-water wave steepness and the spectral wave steepness based on measured wave data from the Norwegian continental shelf, which, therefore, is related to the Hsu (1974) sea surface roughness.

The sea surface roughness enters in the description of the local wind conditions over the sea surface, i.e. using a logarithmic mean wind speed profile plus a wind gust spectrum; see, e.g. Myrhaug and Ong (2009) who investigated the wave age effect on wind gust spectra for wind waves. Many wind gust spectra have been proposed, see, e.g. Chakrabarti (1990). It is well established that wind gust spectra over sea contain more energy at lower frequencies than those over land [see, e.g. Ochi and Shin (1988), Andersen and Løvseth (2006)]. This spectral property is essential when assessing the response, e.g. of moored ships and structures which are sensitive to excitations at low frequencies.

The main purpose and the novelty of the present article is to demonstrate how the Myrhaug and Fouques (2008) bivariate statistics of the spectral wave steepness and the significant wave height representing wind sea, swell, and combined wind sea and swell can be used to obtain statistical properties of the sea surface roughness for sea states given by Taylor and Yelland (2001), which are best to use for mixed wind sea and swell and for swell-dominated situations. This is relevant to the assessment of local wind conditions at sea, e.g. related to wind load studies on marine structures. The Taylor and Yelland (2001) sea surface roughness is adopted due to its compromise between simplicity and robustness. It is also demonstrated how these results affect the local wind conditions described by the logarithmic mean wind speed profile plus the Ochi and Shin (1988) wind gust spectrum. An example of the application is also included.

This article is structured as follows: this section is followed by Sect. 2 describing the background of the Taylor and Yelland (2001) sea surface roughness formula, the logarithmic mean wind speed profile, and the Ochi and Shin (1988) wind gust spectrum. Section 3 presents the application of the Myrhaug and Fouques (2008) bivariate statistics of the spectral wave steepness and the significant wave height by yielding some probabilistic features of sea surface roughness (Sect. 3.1); sea surface drag coefficient and turbulence energy density (Sect. 3.2); estimation of sea surface roughness from n-year return period contour lines (Sect. 3.3); an application related to the effect of the sea surface roughness on slowly varying surge motion of marine structures exposed to wind gust (Sect. 3.4). A summary is provided in Sect. 4.

2 Background

Following Taylor and Yelland (2001), the sea surface roughness is given as

$$\frac{z_0}{H_s} = c\, s_p^d\ ; \quad (c, d) = (1200,\ 4.5), \tag{1}$$

where H_s is the significant wave height, $s_p = H_s/((g/2\pi)T_p^2)$ is the spectral wave steepness, g is the acceleration of gravity, and T_p is the spectral peak period. According to Drennan et al. (2005), Eq. (1) is good for conditions representing mixed wind sea and swell and swell-dominated conditions for $s_p > 0.02$. As referred to in Sect. 1, Zhao and Li (2019) found that z_0 in terms of s_p and H_s can be applied to estimate wind stress for wind sea from low to high winds, i.e. to use Eq. (1) with $(c,\ d) = (2.79,\ 2.77)$.

The mean wind speed profile for a neutrally stable atmospheric boundary layer (i.e. by neglecting temperature gradient effects, which is the case for strong wind) is described by the logarithmic profile

$$\frac{U(z)}{U_{10}} = 2.5\sqrt{C_{10}}\ln\frac{z}{z_0}, \tag{2}$$

where $U(z)$ is the horizontal mean wind speed at the elevation z above the sea surface, z is the vertical coordinate with $z = 0$ at the sea surface and positive upwards, U_{10} is the mean wind speed at $z = 10$ m and $C_{10} = (u_*/U_{10})^2$ is the sea surface drag coefficient. Now C_{10} and z_0 are related by taking $z = 10$ m in Eq. (2), as

$$C_{10} = 0.16\left(\ln\frac{10}{z_0}\right)^{-2}, \tag{3}$$

where z is given in metres.

The wind gust is modelled as a Gaussian random process and thus described by the wind gust spectrum $S(f)$, with f as the frequency in $Hz{=}s^{-1}$. In this article, the horizontal component of the wind gust component in the same direction as $U_z = U(z)$ is considered, exemplified by adopting the Ochi and Shin (1988) spectrum:

$$S(f_*) = \begin{cases} 583\, f_* & \text{for } 0 \le f_* \le 0.003 \\ \dfrac{420\, f_*^{0.70}}{(1 + f_*^{0.35})^{11.5}} & \text{for } 0.003 \le f_* \le 0.1 \\ \dfrac{838\, f_*}{(1 + f_*^{0.35})^{11.5}} & \text{for } 0.1 \le f_* \end{cases}, \tag{4}$$

where the dimensionless frequency is $f_* = f z/U_z$ and the dimensionless spectrum is $S(f_*) = f\, S(f)/u_*^2$, which also is valid for neutrally stable atmospheric conditions. Further-

more, here $f\,S(f)$ is the turbulence energy density, which can be expressed in dimensionless form as

$$\frac{f\,S(f)}{U_{10}^2} = C_{10}S(f_*) \tag{5}$$

using $u_*^2 = C_{10}U_{10}^2$.

The results of using these local wind formulae are elaborated further in Sect. 3.

3 Use of the Myrhaug and Fouques (2008) bivariate statistics of H_s and s_p

3.1 Some statistical features of z_0

Here the Myrhaug and Fouques (2008) (hereafter referred to as MF08) joint probability density function *(pdf)* of H_s and s_p will be used. This *pdf* originates from best fit to data from the northern North Sea representing wave states containing wind sea, swell, and combined wind sea and swell. Thus, there is consistency in using this *pdf* and Eq. (1) since both represent similar wave conditions. It should be noted that the results presented in Sect. 3.1–3.3 are solely based on wave statistics. However, use of these results involving U_{10} should be for U_{10} less than about 30 m/s.

The MF08 joint *pdf* is given as

$$p(H_s, s_p) = p(s_p|H_s)p(H_s), \tag{6}$$

where $p(H_s)$ is the marginal *pdf* of H_s given as a combined lognormal and Weibull distribution (see Eq. (2) in MF08), and $p(s_p|H_s)$ is the conditional *pdf* of s_p given H_s, given as the lognormal *pdf*:

$$p(s_p|H_s) = \frac{1}{\sqrt{2\pi}\sigma s_p}\exp\left[-\frac{(\ln s_p - \mu)^2}{2\sigma^2}\right]. \tag{7}$$

The conditional expected value μ and the conditional variance σ^2 of $\ln s_p$ are

$$\mu = \ln\left(\frac{H_s}{g/2\pi}\right) - 2\left(a_1 + a_2\,H_s^{a_3}\right), \tag{8}$$

$$(a_1,\ a_2,\ a_3) = (1.780,\ \ 0.288,\ \ 0.474), \tag{9}$$

$$\sigma^2 = b_1 + b_2\,e^{b_3\,H_s}, \tag{10}$$

$$(b_1,\ \ b_2,\ \ b_3) = (0.001,\ \ 0.097,\ \ -0.255). \tag{11}$$

Here H_s is in metres in Eqs. (8) and (10) (see MF08 for further background and details).

Now the statistical features of z_0 are derived using this joint *pdf* of H_s and s_p.

First, by a change of variables from $(H_s,\ s_p)$ to $(H_s,\ z_0)$, the joint *pdf* of H_s and z_0 becomes

$$p(H_s, z_0) = p(z_0|H_s)\,p(H_s). \tag{12}$$

Thus, only $p(s_p|H_s)$ is affected since $s_p = (z_0/cH_s)^{\frac{1}{d}}$, which gives a lognormal *pdf* of z_0 given H_s as (i.e. using the Jacobian $|\partial s_p/\partial z_0| = z_0^{\frac{1}{d}-1}/d(cH_s)^{\frac{1}{d}}$)

$$p(z_0|H_s) = \frac{1}{\sqrt{2\pi}\sigma_z z_0}\exp\left[-\frac{(\ln z_0 - \mu_z)^2}{2\sigma_z^2}\right]. \tag{13}$$

The conditional expected value μ_z and the conditional variance σ_z^2 of $\ln z_0$ are

$$\mu_z = d\mu + \ln(cH_s), \tag{14}$$

$$\sigma_z^2 = (d\sigma)^2, \tag{15}$$

where μ and σ are given in Eqs. (8), (9) and (10), (11), respectively.

Second, the conditional expected value and the conditional variance of z_0 are obtained from the known $p(z_0|H_s)$ in Eq. (13) as (Bury 1975)

$$E[z_0|H_s] = \exp\left(\mu_z + \frac{1}{2}\sigma_z^2\right), \tag{16}$$

$$\mathrm{Var}\,[z_0|H_s] = (e^{\sigma_z^2} - 1)\,\exp(2\mu_z + \sigma_z^2). \tag{17}$$

Then it follows that the conditional coefficient of variation is

$$\gamma[z_0|H_s] = \frac{(\mathrm{Var}[z_0|H_s])^{1/2}}{E[z_0|H_s]} = (e^{\sigma_z^2} - 1)^{1/2}. \tag{18}$$

Figure 1 shows the ratio $E[z_0|H_s]/H_s$ versus H_s according to Eq. (16). It appears that this ratio increases as H_s increases, reaching a value of about 0.00032 for $H_s = 15$ m.

Figure 2 shows the conditional coefficient of variation $\gamma[z_0|H_s]$ versus H_s according to Eq. (18). It is seen that $\gamma[z_0|H_s]$ decreases as H_s increases; from values in the range 2–2.5 for small H_s to about 0.3 for $H_s = 15\ m$.

3.2 Conditional statistical values of C_{10} and turbulence energy density

Figure 3 shows the sea surface drag coefficient C_{10} versus H_s according to Eq. (3) by substituting $E[z_0|H_s]$ from Eq. (16) for z_0. It is observed that C_{10} increases as H_s increases, from about 0.005 for small values of H_s up to about 0.0027 for $H_s = 15$ m.

Figure 4 shows $U(z)/U_{10}$ versus z according to Eq. (2) for $H_s = 3$ m, 6 m, 9 m, 12 m. At a given elevation below

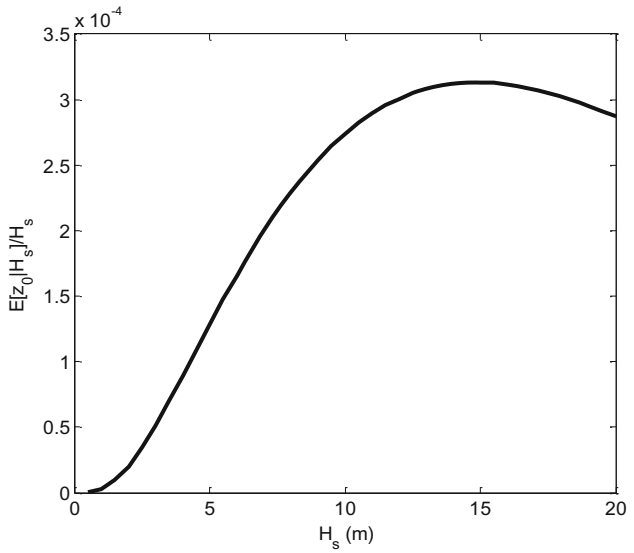

Fig. 1 $E[z_0|H_s]\,/\,H_s$ versus H_s

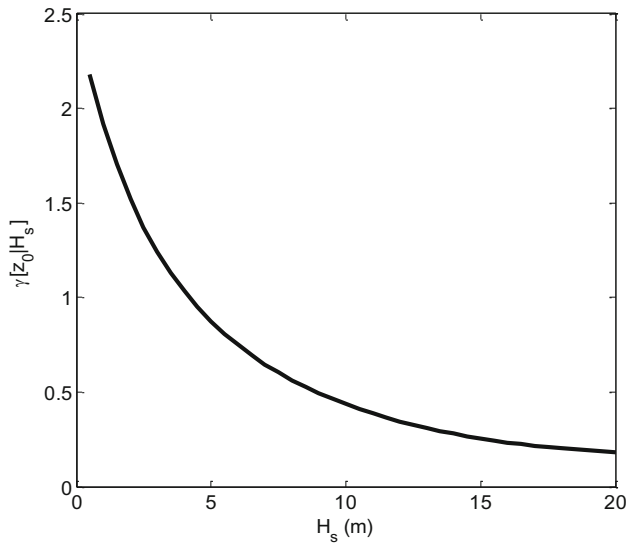

Fig. 2 $\gamma[z_0|H_s]$ versus H_s

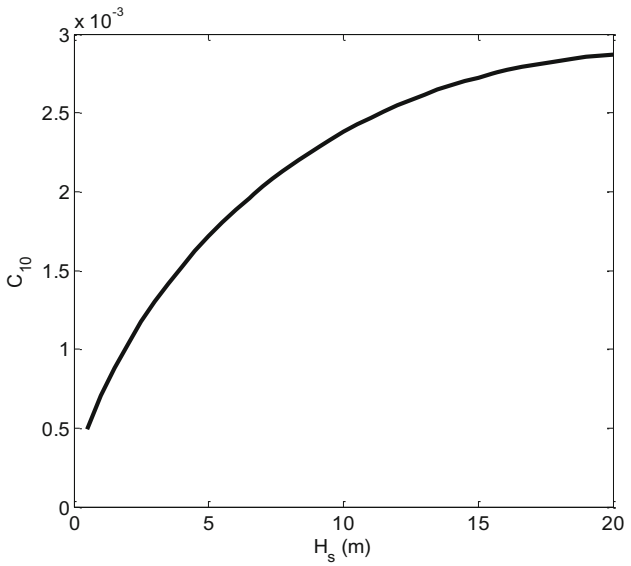

Fig. 3 C_{10} versus H_s

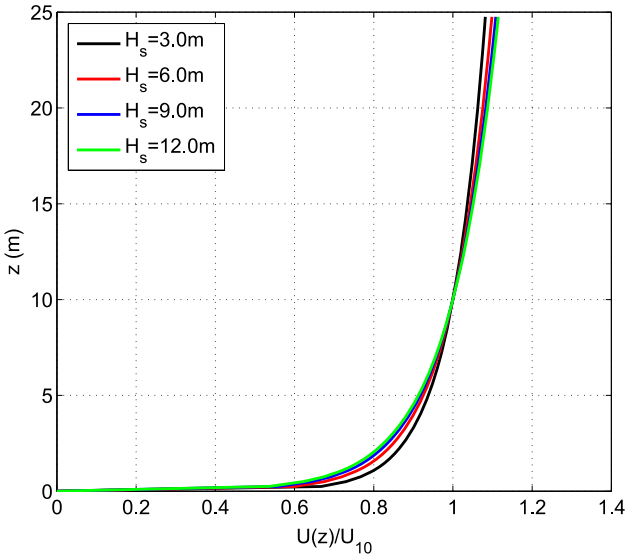

Fig. 4 $U(z)/U_{10}$ versus z for $H_s = 3$ m, 6 m, 9 m and 12 m

$z = 10$ m, it appears that $U(z)/U_{10}$ decreases as H_s increases from 3 m to 12 m, which is due to that the sea surface roughness increases as H_s increases. Moreover, at a given elevation above $z = 10$ m, it is seen that $U(z)/U_{10}$ increases as H_s increases from 3 to 12 m, reflecting that the thickness of the logarithmic boundary layer increases as the sea surface roughness increases.

Figure 5 depicts the dimensionless turbulence energy density $f\ S(f)/U_{10}^2$ as a function of the dimensionless frequency f_* according to Eq. (5) for $H_s = 3$ m, 6 m, 9 m, 12 m, showing the increase of the turbulence energy as H_s increases from 3 to 12 m, i.e. the increase of the turbulence energy density as the sea surface roughness increases.

3.3 Estimation of z_0 based on contour lines of H_s and s_p

Figure 6, which is a re-plotted version of Fig. 13 in MF08, depicts the 1-, 10- and 100-year return period contour lines of H_s and s_p represented by the inner to the outer contours, respectively. MF08 determined these contour lines of H_s, s_p based on a parametric model of a joint *pdf* of H_s and T_p determined from a best fit to deep-water wave data measured in the northern North Sea during a period of 29 years (see MF08 for further details).

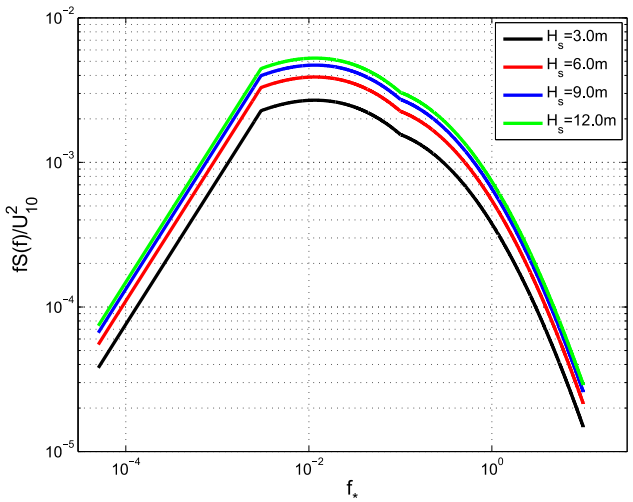

Fig. 5 $f\,S(f)/U_{10}^2$ versus f_* for $H_s = 3$ m, 6 m, 9 m and 12 m

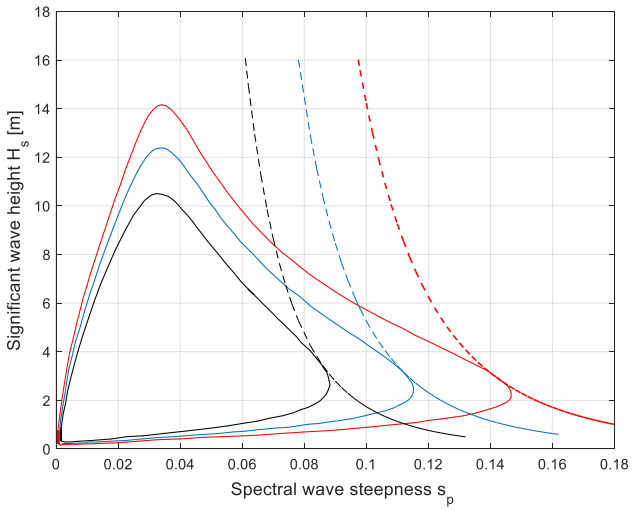

Fig. 6 1-Year, 10-year and 100-year contour lines of H_s and s_p from inner to outer contours, respectively. Tangent lines to the 1-, 10- and 100-year contour lines represent Eq. (19) with the corresponding z_0 values given in Table 1; the corresponding tangent points for H_s, s_p are given in Table 1

Now the information in Fig. 6 is utilized by solving Eq. (1) for H_s, giving

$$H_s = 0.000833\, z_0\, s_p^{-4.5}. \tag{19}$$

For a given value of z_0, this is a curve in the (H_s, s_p) plane. The values of z_0 imply that these curves will have tangent points with the 1-year, the 10-year and the 100-year contours, which can be determined by iteration, and thus the corresponding tangent points. The results are shown graphically in Fig. 6 by the three curves giving tangent points to the 1-, 10- and 100-year contours for $z_0 =$ 0.066 m, 0.20 m, and 0.54 m, respectively. Thus, these values correspond to the 1-, 10- and 100-year return period values of z_0. It is observed that these z_0 values based on the 1-, 10- and 100-year contour lines are governed by s_p since the location of the tangent points is close to the maximum values of s_p along the respective contour lines. The corresponding coordinates of the tangent points for H_s, s_p are given in Table 1, together with the corresponding values of C_{10} (Eq. 3) and T_p, where the latter is obtained from the definition of s_p as

Table 1 The 1-, 10- and 100-year return period values of z_0 and the corresponding values of H_s, s_p, C_{10} and T_p corresponding to the results in Fig. 6

Variable	Return period (years)		
	1	10	100
z_0 (m)	0.066	0.20	0.54
H_s (m)	3.6	3.4	3.1
s_p	0.085	0.11	0.14
C_{10}	0.0064	0.011	0.019
T_p (s)	5.2	4.4	3.8

$$T_p = \left(\frac{2\pi\, H_s}{g\, s_p}\right)^{1/2}. \tag{20}$$

However, one should notice that these values of H_s are far away from the peak values of H_s along the contours, i.e. the peak value of H_s along the 100-year return period contour line is about 14.1 m. It is also noted that the values of s_p are in the validity range of Eq. (1), i.e. $s_p > 0.02$. Furthermore, from Eq. (5), it follows that the turbulence energy density is proportional to C_{10}. Thus, for the same values of U_{10} and f_*, it appears from the values in Table 1 that the ratio between the 10-year and the 1-year values of the turbulence energy density is 1.7; the corresponding ratio between the 100-year and the 1-year values is 3.0.

3.4 Example

Here an example similar to that given in Myrhaug and Ong (2009) is chosen, demonstrating the effect of the 1-, 10- and 100-year return period sea surface roughness values on slowly varying surge motion of structures caused by wind gust. In the Myrhaug and Ong (2009) example, the focus was on demonstrating the wave age effect on wind gust and the consequence for slowly varying surge motion of moored marine structures.

According to Faltinsen (1990), the variance of slowly varying surge motion of moored marine structures caused by wind gust is

$$\sigma_x^2 = \frac{1}{4cb}(C_D A \rho_a U)^2 S(f_N), \tag{21}$$

where c, b, C_D, A, ρ_a, U and f_N denote the restoring coefficient, the damping coefficient, the drag coefficient, the frontal area against the wind, the air density, the mean wind speed and the natural frequency of surge motion, respectively.

The example applies Eq. (21) for U=U_{10} = 20 m/s, z= 10 m, f_N = 0.01 Hz and the Ochi and Shin spectrum in Eq. (4) for the 1-, 10- and 100-year conditions given in Table 1. Since $f_{*N} = 0.01 \times 10/20 = 0.005$, the Ochi and Shin spectrum is given by the formula in Eq. (4) for $0.003 \le f_* \le 0.1$, which gives $S(f_{*N}) = 1.93$ and thus, $S(f_N) = (C_{10}U_{10}^2/f_N)S(f_{*N})$. For the same values of c, b, C_D, A, ρ_a, U_{10} and f_N, it follows that σ_x^2 in Eq. (21) only depends on C_{10}, i.e. on z_0 according to Eq. (3). Consequently, using the results in Table 1, the 10- to 1-year ratio of σ_x^2 is 1.7 and the 100- to 1-year ratio of σ_x^2 is 3.0, i.e. equal to the corresponding ratios for the turbulence energy density given in Sect. 3.3. Although simple, this example demonstrates how the present results can be used, and also illustrates clearly that the response of a moored marine structure that is sensitive to low-frequency excitations depends strongly on the sea surface roughness conditions.

4 Summary

Some statistical features of the Taylor and Yelland (2001) sea surface roughness defined as a function of the spectral wave steepness and the significant wave height are provided using the Myrhaug and Fouques (2008) bivariate statistics of these two sea state wave parameters. Other results for a given sea state include the surface drag coefficient, the logarithmic mean wind speed profile, and the turbulence energy density using the Ochi and Shin (1988) wind gust spectrum.

A procedure to determine the sea surface roughness based on the 1-, 10- and 100-year return period contour lines of H_s and s_p as well as the associated values of H_s and s_p is also given. The presented analytical approach can be applied to estimate the sea surface roughness based on available wave statistics.

Furthermore, an example is provided applying a formula for slowly varying surge motion of moored marine structures to illustrate the effect of wind gust using the 1-, 10- and 100-year return period values of the sea surface roughness as input. It is demonstrated that compared to using the 1-year value of the sea surface roughness, the variance of the surge motion increases by the factors 1.7 and 3.0 using the 10-year and 100-year values of the sea surface roughness, respectively.

Although simple and limited to conditions representing mixed wind sea and swell, as well as swell-dominated conditions for the spectral peak steepness being larger than 0.02, the present results should be useful for the assessment of local wind conditions at sea, e.g. relevant to wind load studies on marine structures. According to Zhao and Li (2019), the sea surface drag coefficient reaches a peak for wind speeds exceeding 30–40 m/s, and thus it is recommended to use the present results for wind speeds less than about 30 m/s.

Acknowledgement Open Access funding provided by NTNU Norwegian University of Science and Technology (incl St. Olavs Hospital - Trondheim University Hospital).

References

Andersen OJ, Løvseth J (2006) The Frøya database and maritime boundary layer wind description. Mar Struct 19:173–192. https://doi.org/10.1016/j.marstruc.2006.007.03

Bury KV (1975) Statistical models in applied science. Wiley, New York

Chakrabarti SK (1990) Non-linear methods in offshore engineering. Elsevier, Amsterdam

Charnock H (1955) Wind stress on a water surface. QJR Meteorol Soc 81:639–640

Donkers JAJ, Brand AJ, Eecen PJ (2011) Offshore wind atlas of the Dutch part of the North Sea. In: Presented at the EWEA 2011, Brussels, Belgium, 14–17 March. https://www.ecn.nl/docs/library/report/2011/m11031.pdf

Drennan WM, Taylor PK, Yelland MJ (2005) Parameterizing the sea surface roughness. J Phys Oceanogr 35:835–848

Faltinsen OM (1990) Sea loads on ships and marine structures. Cambridge University Press, Cambridge

Hsu SA (1974) A dynamic roughness equation and its application to wind stress determination at the air-sea interface. J Phys Oceanogr 4:116–120

Jones ISF, Toba Y (2001) Wind stress over the ocean. Cambridge University Press, Cambridge

Kalverla PC, Steeneveld G-J, Ronda RJ, Holtslag AAM (2017) An observational climatology of anomalous wind events at offshore meteomast IJmuiden (North Sea). J Wind Eng Ind Aerodyn 165:86–99. https://doi.org/10.1016/j.jweia.2017.10.003

Myrhaug D (2018) Some probabilistic properties of deep water wave steepness. Oceanologia 60(2):187–192. https://doi.org/10.1016/j.oceano.2017.10.003

Myrhaug D (2020) Comments regarding "Dependence of wind stress across an air-sea interface on wave states" by D. Zhao, M. Li. J Oceanogr. https://doi.org/10.1007/s10872-018-0494-9

Myrhaug D, Fouques S (2008) Bivariate distributions of significant wave height with characteristic wave steepness and characteristic surf parameter. In: Proc 27th Int Conf. on Offshore Mech and Arctic Eng, Estoril, Portugal, Paper No. OMAE2008-57728

Myrhaug D, Ong MC (2009) Effect of wave age on wind gust spectra over wind waves. ASME J Offshore Mech Arctic Eng 131:034501-1–034501-6

Ochi MK, Shin YS (1988) Wind turbulent spectra for design considerations of offshore structures. In: Proc 20th Offshore Tech Conf, Houston, Texas, Paper No 5736 1;461-467

Powell MD, Vickery PJ, Reinhold TA (2003) Reduced drag coefficient for high wind speeds in tropical cyclones. Nature 422:279–283

Taylor PK, Yelland MJ (2001) The dependence of sea surface roughness on the height and steepness of the waves. J Phys Oceanogr 31:572–590

Zhao D, Li M (2019) Dependence of wind stress across an air-sea interface on wave states. J Oceanogr 75(3):207–223. https://doi.org/10.1007/s10872-018-0494-9